

## Experimental and Theoretical Evaluation of Asymmetric Thioureas on the Corrosion of Carbon Steel in Acidic Medium

Arthur Valbon<sup>1</sup>, Marcelo. A. Neves<sup>2</sup>, Aurea Echevarria<sup>1,\*</sup>

<sup>1</sup> Departamento de Química, Instituto de Ciências Exatas, Universidade Federal Rural do Rio de Janeiro, 23890-000, Seropédica – Rio de Janeiro, Brasil

<sup>2</sup> Departamento de Física, Instituto de Ciências Exatas, Universidade Federal Rural do Rio de Janeiro, 23890-000, Seropédica – Rio de Janeiro, Brasil

\*E-mail: [echevarr@ufrj.br](mailto:echevarr@ufrj.br)

Received: 25 January 2017 / Accepted: 23 February 2017 / Published: 12 March 2017

---

The inhibitory effects of *N*-(*p*-X-phenyl)-*N*'-benzyl-thiourea (THIOB1 and THIOB2) and *N*-(*p*-X-phenyl)-*N*'-phenethyl-thiourea (THIOF1 and THIOF2) on the corrosion of AISI 1020 carbon steel in 1 mol L<sup>-1</sup> HCl were evaluated by polarization curves (PP), Linear Polarization Resistance (LPR), Electrochemical Impedance Spectroscopy (EIS) and molecular modeling. The corrosion inhibition efficiency of phenethyl-thioureas slightly exceeded that observed for benzyl-thioureas; also, all thioureas acted as mixed inhibitors. 98% was the maximum anticorrosion efficiency for THIOF2, obtained by LPR. The adsorption of the evaluated inhibitors followed Langmuir isotherm. Theoretical results were corroborated by experimental data that showed phenethyl-thioureas were slightly better corrosion inhibitors than benzyl-thioureas.

---

**Keywords:** Carbon steel, Polarization, EIS, Modeling studies, Acid corrosion

### 1. INTRODUCTION

Carbon steel is one of the most important materials in the world and has a wide variety of industrial applications [1]. Acidic solutions are commonly used in industrial processes, such as pickling, acid cleaning and cleaning of oil refinery equipment, even though they accelerate the corrosion of metallic materials and affect the performance of metals subjected to such processes [2]. To overcome the problem, corrosion inhibitors, which can be either organic or inorganic, are widely used in the industrial sector.

The most efficient organic inhibitors used in industry contain oxygen, nitrogen or sulfur atoms. Inhibitors containing multiple bonds also facilitate the adsorption of these compounds onto metal surfaces. A fundamental feature of this type of inhibitor is the bond that can be formed between the electron pair of donor atoms and/or  $\pi$ , thereby reducing corrosive effects in acidic mediums [3-8]. High efficiencies have been observed when the compound has both nitrogen and sulfur atoms [2,5]. Thiourea and its derivatives are among the various classes of compounds with such characteristic, and they have been widely applied as effective corrosion inhibitors for almost fifty years [6-12].

It is well-known that effective corrosion inhibitors must form a stable film by forming coordination bonds between the heteroatoms of the inhibitors and Fe on the metallic surface. The stability of these films depends mainly on the type of interaction between the inhibitor and the metal surface, which is related to the chemical structure of the inhibitor (i.e. functional groups, aromaticity, steric effects and electronic density of the donor atoms). The corrosive environment also plays an important role in this issue [13]. The molecule polar group is usually regarded as the chelation centre for the establishment of the adsorption process on the metal surface [14].

In a recent study of anticorrosion activity, 1,3-bis-(morpholin-4-yl-phenyl-methyl)-thiourea showed good results at various hydrogen chloride concentrations in acidic mediums; the corrosion inhibition efficiency reached 93% in 5% HCl in aqueous solution [15].

Allylthiourea is also studied as a highly efficient corrosion inhibitor for steel, reaching 95% efficiency in acidic medium of  $\text{H}_3\text{PO}_4$  [2].

Recently, Finšgar and Jackson, 2014, have reported the inhibition efficiency of three tested thioureas: 1,3-dibutyl-2-thiourea, 1,3-diethyl-2-thiourea, and 1,3-dimethyl-2-thiourea (95%, 88%, and 70%, respectively), in the presence of formaldehyde 0.6% (w/v) in acidic medium of 10% HCl (w/v) [16].

The molecular modeling technique has been extensively used to correlate corrosion inhibition efficiency with theoretical parameters [10,11]. Structural parameters, such as the energies of the frontier molecular orbitals HOMO (Highest Occupied Molecular Orbital), LUMO (Lowest Unoccupied Molecular Orbital), as well as the dipole moment influence the potential inhibition and generally show strong correlation with experimentally determined inhibitory effects [17-20].

Papers involving the anticorrosion activity of thioureas generally showed complex molecular structures [15], an acidic medium of  $\text{H}_3\text{PO}_4$  [2], or thioureas in mixtures [16], among other things. Therefore, this work evaluated the inhibitory effects of *N*-(*p*-X-phenyl)-*N'*-benzyl-thiourea (THIOB1 and THIOB2) and *N*-(*p*-X-phenyl)-*N'*-phenethyl-thiourea (THIOF1 and THIOF2) (where X = H and  $\text{OCH}_3$ ), synthesized by a new method using ultrasonic irradiation on AISI 1020 carbon steel in 1 mol  $\text{L}^{-1}$  HCl, employing Potentiodynamic Polarization (PP), Linear Polarization Resistance (LPR) and Electrochemical Impedance Spectroscopy (EIS). Furthermore, the results were compared with theoretical parameters, such as the highest occupied molecular orbital energy ( $E_{\text{HOMO}}$ ), the lowest unoccupied molecular orbital energy ( $E_{\text{LUMO}}$ ), Mulliken charges, and the dipole moment ( $\mu$ ), obtained by semi-empirical method, PM3, Spartan-PRO program.

## 2. EXPERIMENTAL

### 2.1. Synthesis

#### 2.1.1. *N*-(*p*-X-phenyl)-*N'*-benzyl-thiourea (THIOB1 and THIOB2) and *N*-(*p*-X-phenyl)-*N'*-phenethyl-thiourea (THIOF1 and THIOF2)

The selected amine (benzylamine or phenethylamine) was added to a solution of phenylisothiocyanate or 4-methoxy-phenylisothiocyanate, previously dissolved in chloroform. The reaction mixture was placed into an ultrasonic bath at room temperature for 20 minutes. The product was collected by filtration and washed with cold chloroform. Benzyl-thioureas (THIOB1 and THIOB2) were obtained with 89-95% yield [21], and the phenethyl-thioureas (THIOF1 and THIOF2), with 90-98% yield [22-24]. Fig. 1 shows the structures of the synthesized thioureas.

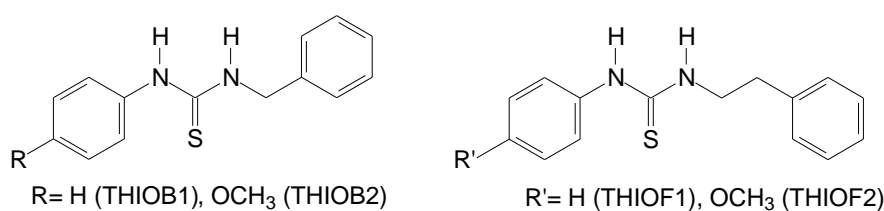


**Figure 1.** Chemical structures of synthesized and tested *N*-(*p*-X-phenyl)-*N'*-benzyl-thiourea and *N*-(*p*-X-phenyl)-*N'*-phenethyl-thiourea.

### 2.2. Electrochemical measurements

#### 2.2.1. Solution preparation

Stock thiourea solutions were prepared in an ethanol/water (7:3) mixture for complete solubilisation, after being diluted in the following concentrations: 0 (blank),  $2.5 \times 10^{-5}$ ,  $1.0 \times 10^{-5}$ ,  $1.0 \times 10^{-6}$  and  $1.0 \times 10^{-7}$  mol L<sup>-1</sup> in HCl 1.0 mol L<sup>-1</sup>.

#### 2.2.2. Electrochemical tests

The tests were carried out at room temperature using a conventional electrochemical three-electrode cell, containing carbon steel working electrode, platinum auxiliary electrode and silver-silver chloride (Ag/AgCl, 3.0 mol L<sup>-1</sup> KCl) reference electrode. The working electrode was prepared from AISI 1020 carbon steel with the following composition (wt.%): C: 0.17, P: 0.04, S: 0.05, Mn: 0.30, Si: trace and the remainder Fe. The electrode was prepared by embedding the steel rods in epoxy resin and exposing a surface area of 0.8 cm<sup>2</sup>. Before each measurement, the steel surface was abraded with 600, 800 and 1200 grade emery paper, washed with triply-distilled water, degreased with ethanol and dried [12]. The electrolyte was 1 mol L<sup>-1</sup> HCl, and all experiments were carried out in 40 mL solutions of naturally aerated electrolyte at 25 °C.

All electrochemical measurements were performed in triplicate, using AC signals, and realized at open circuit potential (OCP) for 40 minutes to be sufficient to attain a stable state; the measurements were taken using Autolab Potentiostat/Galvanostat PGSTAT 302N and analysed by NOVA 1.9 software.

Impedance measurements were performed over a frequency range of 10 kHz – 10 mHz with a 10 mV peak-to-peak amplitude using AC signal. The inhibition efficiency was calculated using the following equation [13]:

$$\eta_{\text{EIS}}(\%) = \frac{R_{\text{ct}} - R_{\text{ct}}^0}{R_{\text{ct}}} \times 100 \quad (1)$$

where  $R_{\text{ct}}$  is the charge transfer resistance in the presence of the inhibitor, and  $R_{\text{ct}}^0$  is the charge transfer resistance in the absence of the inhibitor.

Linear Polarization Resistance experiments were performed using a scan rate of  $1\text{mV}\cdot\text{s}^{-1}$  in the potential range of  $\pm 10$  mV around the open circuit potential ( $E_{\text{ocp}}$ ). The inhibition efficiency was calculated using the following equation [25]:

$$\eta_{\text{LPR}}(\%) = \frac{R_{\text{p}} - R_{\text{p}}^0}{R_{\text{p}}} \times 100 \quad (2)$$

where  $R_{\text{p}}$  and  $R_{\text{p}}^0$  are the polarization resistance in the presence and absence of the inhibitor, respectively. The polarization resistance was obtained through the following equation [14,25]:

$$R_{\text{p}} = \frac{\Delta E}{\Delta i} \quad (3)$$

determined by graphing the current ( $I$ ) vs the potential ( $E$ ), where  $R_{\text{p}}$  is the slope of the line.

Potentiodynamic anodic and cathodic polarization curves were performed using a scan rate equal to  $1\text{ mV s}^{-1}$  from  $-200$  mV up to  $+200$  mV around the open circuit potential [13, 26].

## 2.3. Surface analysis

### 2.3.1. Scanning electron microscopy (SEM)

Carbon steel test samples, dimension  $4\text{ cm} \times 5\text{ cm} \times 0.1\text{ cm}$ , were abraded with 600, 800 and 1200 grade emery paper, washed with triply-distilled water and ethanol, dried and immersed in  $1\text{ mol L}^{-1}\text{HCl}$  in the absence (Blank) and presence of the inhibitor (THIOF2) for 2 hours at room temperature. The specimens were removed, washed with triply-distilled water, ethanol and dried. The measurements were taken using HITACHI TM 3000 Tabletop Microscope [12].

## 2.4. Molecular modelling

Calculations were performed using semi-empirical method PM3 (Parameterized Model Number 3) of Spartan-14 program [27-29]. The energies of HOMO and LUMO, the energy gap

between them ( $\Delta E_{\text{LUMO-HOMO}}$ ), the ionization energies, the dipole moments ( $\mu$ ), the Mulliken charges, and the HOMO and LUMO orbitals were obtained for all the thioureas synthesized in this work [30].

### 3. RESULTS AND DISCUSSION

#### 3.1. Potentiodynamic polarization measurements

Fig. 2 presents the potentiodynamic polarization curves of carbon steel in  $1 \text{ mol L}^{-1}$  HCl solutions with and without thioureas THIOB1-2 and THIOF1-2 at different concentrations at  $25 \text{ }^\circ\text{C}$ . According to the polarization curves, the presence of all compounds promotes a remarkable decrease in the corrosion rate in the anodic and cathodic current, mainly with higher concentrations of the inhibitors, and an intense shift of the  $E_{\text{CORR}}$  in the anodic direction. These results indicate that these compounds acted as mixed-type corrosion inhibitors that could retard metal dissolution and the cathodic process. In addition, these compounds acted as adsorption inhibitors, meaning that more molecules were adsorbed on the metal surface as the concentration increased, promoting better surface coverage [31].

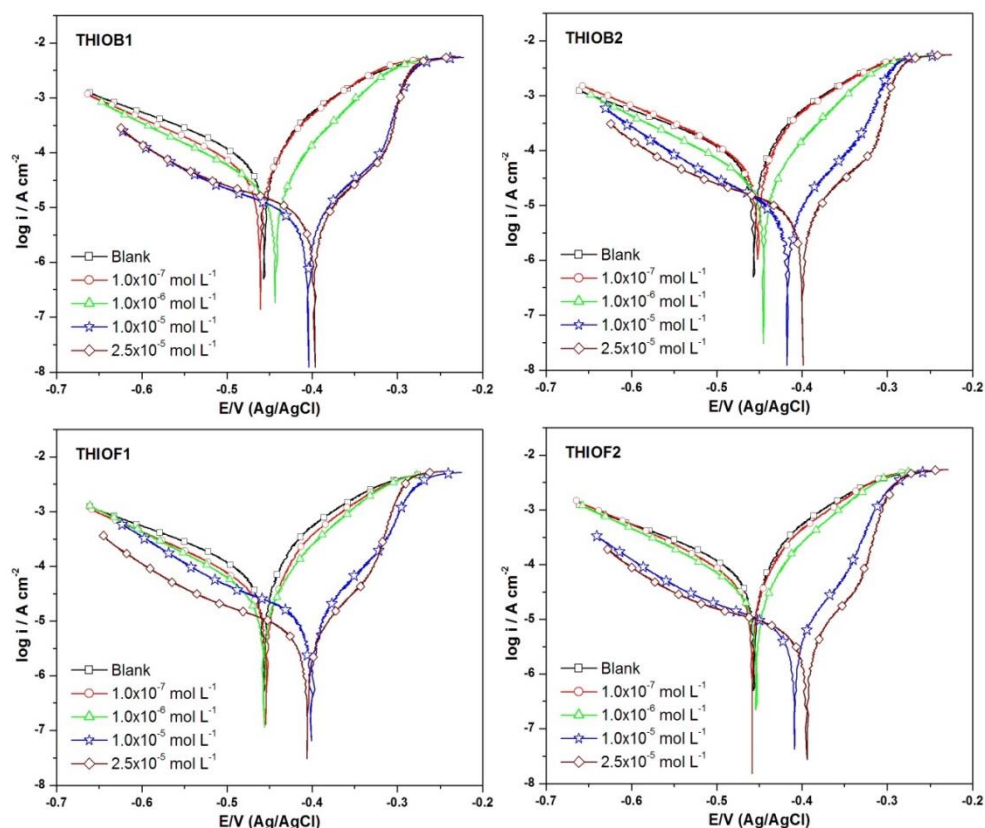


**Figure 2.** Polarization curves of carbon steel in  $1.0 \text{ mol L}^{-1}$  HCl in the presence and absence of benzylthioureas (THIOB1-2) and phenetylthioureas (THIOF1-2).

In Table 1, it is possible to observe electrochemical parameters like the corrosion potential ( $E_{\text{corr}}$ ), the corrosion current density ( $j_{\text{corr}}$ ), and the anodic ( $\beta_a$ ) and cathodic ( $\beta_c$ ) Tafel constants, obtained by the Tafel plots. Through the  $j_{\text{corr}}$  values obtained in the presence and absence of compounds THIOB1-2 and THIOF1-2, it was possible to calculate the inhibition efficiency.

**Table 1.** Electrochemical parameters obtained from carbon steel Polarization Potentiodynamic measurements in the presence and absence of different inhibitor concentrations in 1.0 mol L<sup>-1</sup> HCl.

Inhibitor	$C_{\text{inh}}$ (mol L <sup>-1</sup> )	$E_{\text{corr}}$ vs. Ag/AgCl (mV)	$j_{\text{corr}}$ ( $\mu\text{A cm}^{-2}$ )	$\beta_a$ (mV dec <sup>-1</sup> )	$-\beta_c$ (mV dec <sup>-1</sup> )	$\theta$	$\eta_{\text{PP}}$ (%)
Blank	-	-457	94.6	165	61	-	-
THIOB1	$1.0 \times 10^{-7}$	-455	42.5	158	58	0.55	55
	$1.0 \times 10^{-6}$	-444	27.8	129	51	0.71	71
	$1.0 \times 10^{-5}$	-406	10.9	234	85	0.88	88
	$2.5 \times 10^{-5}$	-398	12.9	248	89	0.86	86
THIOB2	$1.0 \times 10^{-7}$	-453	70.2	129	48	0.26	26
	$1.0 \times 10^{-6}$	-432	34.0	148	60	0.64	64
	$1.0 \times 10^{-5}$	-426	10.5	168	74	0.89	89
	$2.5 \times 10^{-5}$	-409	5.7	88	48	0.94	94
THIOF1	$1.0 \times 10^{-7}$	-455	56.5	161	56	0.40	40
	$1.0 \times 10^{-6}$	-458	37.8	121	61	0.60	60
	$1.0 \times 10^{-5}$	-410	10.3	173	56	0.89	89
	$2.5 \times 10^{-5}$	-407	9.1	217	77	0.90	90
THIOF2	$1.0 \times 10^{-7}$	-459	55.3	124	54	0.42	42
	$1.0 \times 10^{-6}$	-455	42.0	126	60	0.56	56
	$1.0 \times 10^{-5}$	-410	6.7	138	55	0.93	93
	$2.5 \times 10^{-5}$	-395	5.6	142	63	0.94	94

### 3.2. Linear polarization resistance measurements

Linear Polarization Resistance to carbon steel in HCl 1 mol L<sup>-1</sup> were evaluated in the presence and in absence of thioureas THIOB 1-2 and THIOF 1-2.  $R_p$  was obtained by graphing current ( $i$ ) vs potential ( $E$ ), where  $R_p$  is the slope of the line. Table 2 shows that the slope increases with the inhibitor concentration; thus, compounds that show higher  $R_p$  values are more effective for corrosion inhibition.

**Table 2.** Electrochemical parameters obtained from carbon steel LPR measurements in the presence and absence of different inhibitor concentrations in 1.0 mol L<sup>-1</sup> HCl.

Inhibitor	C <sub>inh</sub> (mol L <sup>-1</sup> )	R <sub>p</sub> (Ω cm <sup>2</sup> )	θ	η <sub>LPR</sub> (%)
Blank	-	180.22	-	-
THIOB1	1.0x10 <sup>-7</sup>	414.70	0.5654	57
	1.0x10 <sup>-6</sup>	566.13	0.6817	68
	1.0x10 <sup>-5</sup>	4024.03	0.9552	95
	2.5x10 <sup>-5</sup>	3993.80	0.9549	95
THIOB2	1.0x10 <sup>-7</sup>	346.56	0.4800	48
	1.0x10 <sup>-6</sup>	579.78	0.6892	69
	1.0x10 <sup>-5</sup>	1747.74	0.8969	90
	2.5x10 <sup>-5</sup>	3433.18	0.9475	95
THIOF1	1.0x10 <sup>-7</sup>	423.66	0.5746	57
	1.0x10 <sup>-6</sup>	515.57	0.6504	65
	1.0x10 <sup>-5</sup>	2135.86	0.9156	92
	2.5x10 <sup>-5</sup>	3433.18	0.9475	95
THIOF2	1.0x10 <sup>-7</sup>	368.50	0.5109	51
	1.0x10 <sup>-6</sup>	513.84	0.6493	65
	1.0x10 <sup>-5</sup>	2053.21	0.9128	91
	2.5x10 <sup>-5</sup>	8486.60	0.9788	98

According to the data presented in Table 2, the highest inhibition efficiency was 98% for compound THIOF2 at the maximum tested concentration (2.5x10<sup>-5</sup> mol L<sup>-1</sup>). This might be related to the presence of the methoxy group, an electron donor and two methylene carbons in compound THIOF2.

### 3.3. Electrochemical impedance spectroscopy measurements

Nyquist plots of the carbon steel electrode in HCl 1 mol L<sup>-1</sup> with and without the addition of compounds THIOB1-2 and THIOF1-2 at different concentrations are shown in Fig. 3. Nyquist plots show a single capacitive semicircle for the blank and inhibitor agent solutions. As shown in Fig. 4, the semicircle increases with the thiourea concentration, and there is consequently a gain in the inhibition efficiency. This indicates that the corrosion of carbon steel in acidic medium is controlled by a charge-transfer process [8]. The charge-transfer resistance values ( $R_{ct}$ ) were obtained from  $Z_{real}$  on the x-axis, where the intersection at high-frequency corresponds to the ohmic resistance of the solution ( $R_s$ ), and the intersection at low-frequency corresponds to  $R_{ct}+R_s$ . Therefore, the  $R_{ct}$  values were calculated through the difference between  $R_{ct}+R_s$  and  $R_s$  [13,32].

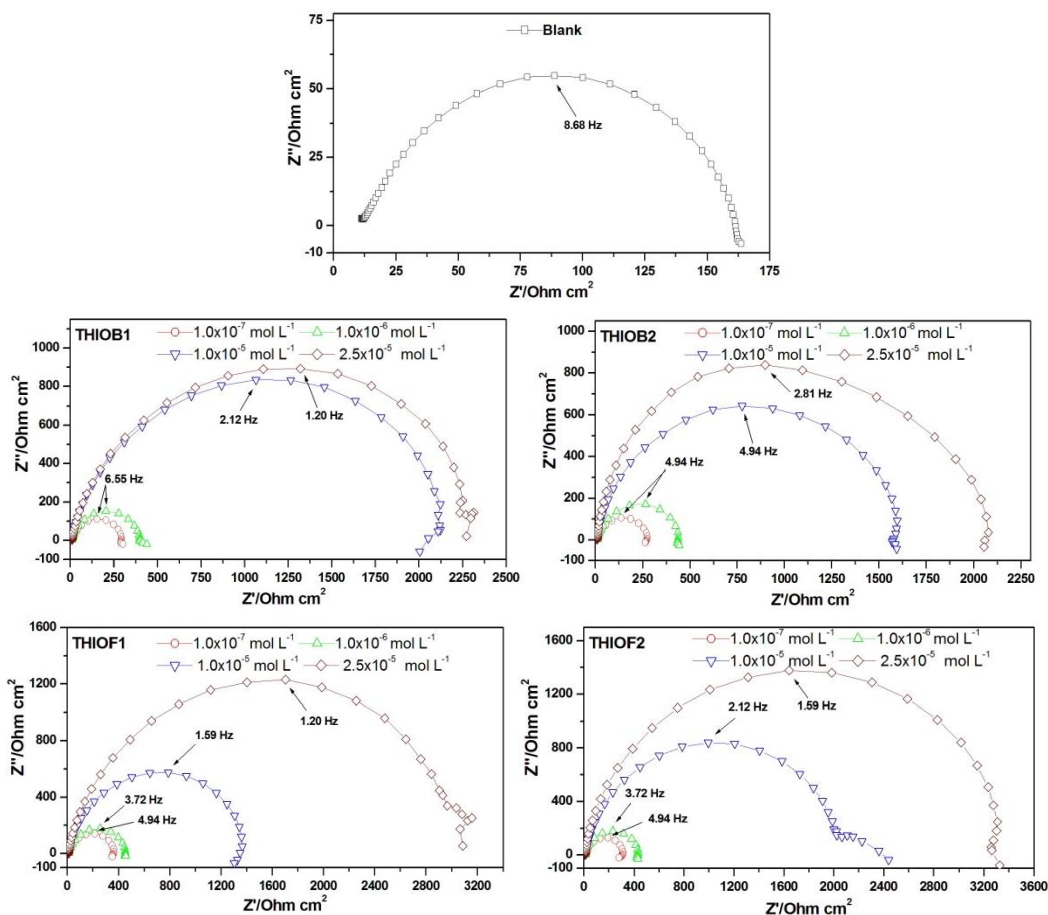


**Figure 3.** Nyquist plots of carbon steel obtained in HCl 1.0 mol L<sup>-1</sup> in the presence and absence of benzyl-thioureas (THIOB1-2) and phenetyl-thioureas (THIOF1-2).

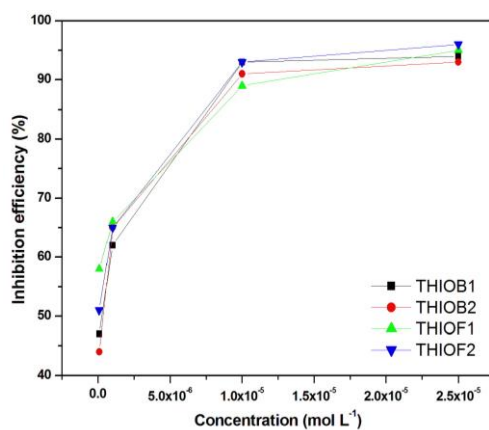


**Figure 4.** Variation of the inhibition efficiency with concentration.

The double layer capacitance ( $C_{dl}$ ) was evaluated as follows:

$$C_{dl} = \frac{1}{2\pi f_{max}R_{ct}} \tag{4}$$

where  $f_{max}$  is the frequency value at which the imaginary component is maximum. The increase of  $R_{ct}$  and the decrease of  $C_{dl}$  indicates that these thioureas inhibit the corrosion rate of carbon steel by adsorption mechanisms [33].

Fig. 5 illustrates the equivalent circuit fitted with error below 6%, used to analyse all the EIS spectra, corroborating with the experimental results [12,34-36]. Compounds are represented from the simplest fitting equivalent circuit, which is a parallel combination of the charge-transfer resistance ( $R_{ct}$ ) and the double-layer capacitance ( $C_{dl}$ ), both in series with the solution resistance ( $R_s$ ) [33].

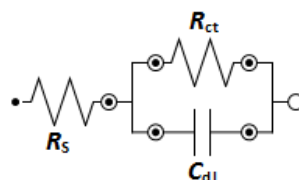


**Figure 5.** The equivalent circuit models used to fit EIS experimental data, simple equivalent circuit for THIOB1-2 and THIOF1-2.

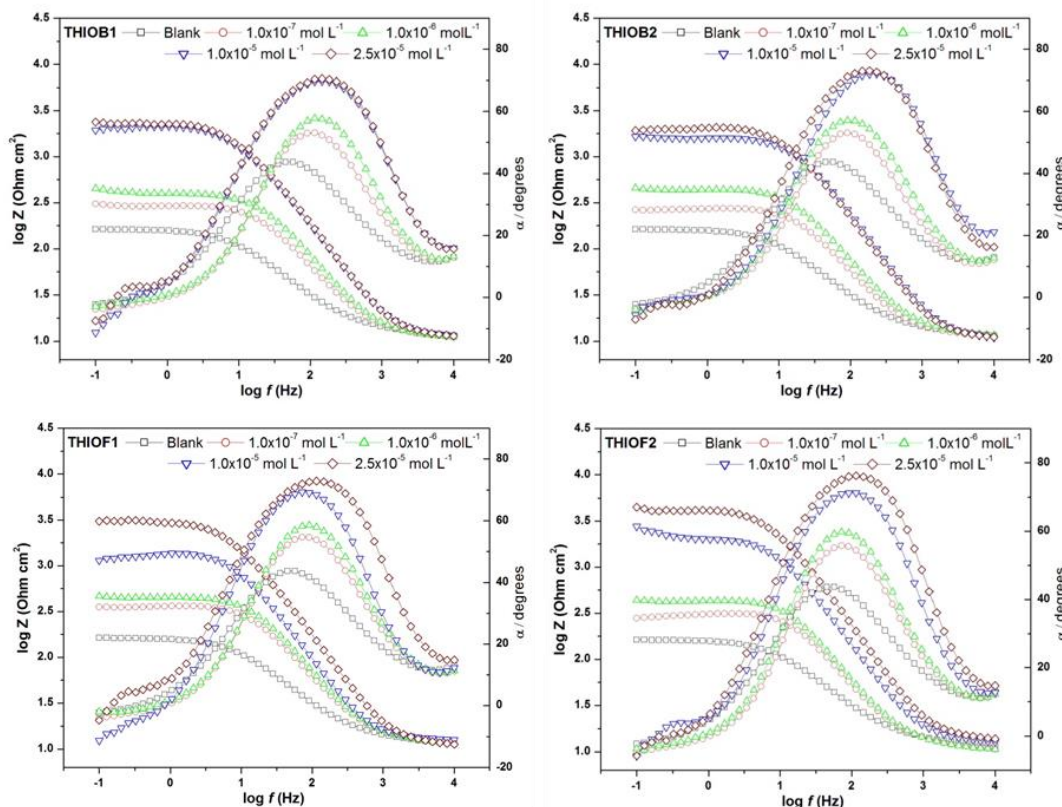


**Figure 6.** Bode plots of carbon steel obtained in  $1.0 \text{ mol L}^{-1}$  HCl in the presence and absence of benzyl-thioureas (THIOB1-2) and phenetyl-thioureas (THIOF1-2).

Bode plots for carbon steel in acidic media with and without inhibitors are shown in Fig. 6. At low frequencies,  $Z_{mod}$  is a metric that can be used to compare the corrosion resistance of different samples. An increase in  $Z_{mod}$  leads to better inhibitory performance [36]. According to Fig. 6,  $Z_{mod}$  increases when the inhibition efficiency raises, and so does the inhibitor concentration.

Table 3 shows values of  $R_{ct}$ ,  $C_{dl}$ , and the efficiency of corrosion inhibition for THIOB1-2 and THIOF1-2. The best corrosion inhibition efficiency recorded by EIS was 96% for phenethyl-thiourea THIOF2 at the maximum concentration ( $2.5 \times 10^{-5}$  mol L<sup>-1</sup>); low  $C_{dl}$  values were also observed. The decrease in  $C_{dl}$  values may be caused by a decline in the dielectric constant, and/or an increase in the thickness of the electrical double layer, thus indicating that the inhibitors function by adsorption at the metal surface [13]. The presence of methoxy moiety in THIOF2, given the electron donor effect of the resonance, increased the electronic density in the centre of the potential adsorption atom, sulfur.

**Table 3.** Electrochemical impedance data for carbon steel in 1.0 mol L<sup>-1</sup> HCl at different inhibitor concentrations.

Inhibitors	$C_{inh}$ (mol L <sup>-1</sup> )	OCP/ Ag/AgCl (mV)	$R_{ct}$ ( $\Omega$ cm <sup>2</sup> )	$C_{dl}$ ( $\mu$ F cm <sup>-2</sup> )	$\theta$	$\eta_{EIS}$ (%)
Blank	-	-461	149.53	122.62	-	-
THIOB1	$1.0 \times 10^{-7}$	-466	281.24	86.40	0.4683	47
	$1.0 \times 10^{-6}$	-450	389.43	62.39	0.6160	62
	$1.0 \times 10^{-5}$	-411	2144.72	35.00	0.9303	93
	$2.5 \times 10^{-5}$	-421	2323.52	57.08	0.9356	94
THIOB2	$1.0 \times 10^{-7}$	-464	265.85	121.19	0.4375	44
	$1.0 \times 10^{-6}$	-451	423.99	75.98	0.6473	65
	$1.0 \times 10^{-5}$	-475	1589.60	20.26	0.9059	91
	$2.5 \times 10^{-5}$	-420	2101.36	26.95	0.9288	93
THIOF1	$1.0 \times 10^{-7}$	-459	353.27	91.20	0.5767	58
	$1.0 \times 10^{-6}$	-459	438.87	97.48	0.6593	66
	$1.0 \times 10^{-5}$	-425	1361.36	73.52	0.8902	89
	$2.5 \times 10^{-5}$	-445	3182.48	41.67	0.9530	95
THIOF2	$1.0 \times 10^{-7}$	-463	305.34	105.51	0.5103	51
	$1.0 \times 10^{-6}$	-457	423.53	101.01	0.6469	65
	$1.0 \times 10^{-5}$	-473	2050.56	36.61	0.9271	93
	$2.5 \times 10^{-5}$	-428	3335.28	30.01	0.9552	96

In general, phenethyl-thioureas had slightly higher corrosion inhibition efficiencies, which can be correlated with the presence of two methylene groups. These groups alter the spatial structure and yield better planarity and hydrophobicity when compared with benzyl-thiourea. This contributes to superior inhibitor/surface interaction and the expulsion of water molecules from the surface. Further, the no observation of dependence of inhibitor concentration with anticorrosion efficiency, should be related to high adsorption of thiourea in surface at all concentrations.

The results obtained in this study were better when compared with similar compounds in literature, for instance, Torres *et al.* obtained maximum efficiency of 96% at  $1.0 \times 10^{-4}$  mol L<sup>-1</sup> inhibitor in 1 mol L<sup>-1</sup> HCl using dibenzil thiourea (DBTU) [12], whereas at the same conditions, THIOF2

showed 98% of efficiency at  $2.5 \times 10^{-5} \text{ mol L}^{-1}$ . Also, Quraishi *et al.* obtained 94.86% at the concentration of 300 ppm ( $2.0 \times 10^{-4} \text{ mol L}^{-1}$ ) of ditolyl thiourea (DTTU) in 20% formic acid [37].

### 3.4. Adsorption isotherm

The type of adsorption isotherm can provide additional information on the properties of the tested compounds. To obtain the adsorption isotherm, various techniques can be used to calculate the degree of the inhibitor surface coverage ( $\theta$ ). In this study, the degree of surface coverage ( $\theta$ ) was calculated by EIS, from the following equation:

$$\theta = \frac{R_{ct} - R_{ct}^0}{R_{ct}} \tag{5}$$

where  $R_{pct}$  and  $R_{ct}^0$  are the Polarization Resistance with and without the inhibitor, respectively.

In accordance with literature, Langmuir isotherm was used to describe the adsorption of thiourea and its derivatives, and it led to a linear correlation coefficient close to 1. Fig. 7 shows the fit of the obtained data to the Langmuir isotherm by plotting  $C_{inh}/\theta$  versus  $C_{inh}$ , according to the equation:

$$\frac{C_{inh}}{\theta} = \frac{1}{K_{ads}} + C_{inh} \tag{6}$$

where  $C_{inh}$  is the inhibitor concentration,  $\theta$  is the degree of surface coverage and  $K_{ads}$  is the adsorption equilibrium constant. The standard free energy of adsorption ( $\Delta G_{ads}^0$ ) was calculated by the equation below:

$$\Delta G_{ads}^0 = -RT \ln(55.55 K_{ads}) \tag{7}$$

where  $R$  is the universal gas constant ( $\text{J K}^{-1} \text{ mol}^{-1}$ ),  $T$  is the temperature (K), and 55.55 is the molar concentration ( $\text{mol L}^{-1}$ ) of water in the solution.

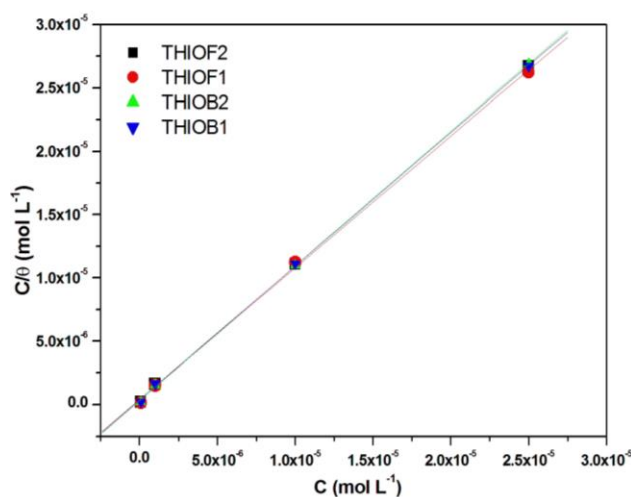


**Figure 7.** Langmuir isotherm plots for the adsorption of benzyl-thioureas (THIOB1-2) and phenethyl-thioureas (THIOF1-2) on carbon steel surface in HCl 1.0 mol L<sup>-1</sup>.

The thermodynamic parameters obtained are listed in Table 4, where a high linear correlation coefficient ( $r$ ) and a slope near to 1 can be observed, confirming that the adsorption of benzyl and phenetyl-thioureas in a 1 mol L<sup>-1</sup> HCl solution follows the Langmuir adsorption isotherm [12,38].

**Table 4.** Thermodynamic parameters for the adsorption of inhibitors in 1.0 mol L<sup>-1</sup>HCl on carbon steel surface.

Inhibitor	$r$	Slope	$K_{\text{ads}}$ (L mol <sup>-1</sup> )	$\Delta G_{\text{ads}}^0$ (kJ mol <sup>-1</sup> )
THIOB1	0.9998	1.05	$5.75 \times 10^{+5}$	-42.79
THIOB2	0.9999	1.06	$5.16 \times 10^{+5}$	-42.52
THIOF1	0.9996	1.04	$8.49 \times 10^{+5}$	-43.75
THIOF2	0.9998	1.05	$8.49 \times 10^{+5}$	-43.75

The high  $K_{\text{ads}}$  values obtained for all thioureas indicated a strong interaction with the C-steel surface in acidic medium [26], which can be attributed to the presence of nitrogen and sulfur atoms, as well as the  $\pi$ -electrons in each of the studied compounds.

The physisorption phenomenon may be associated with electrostatic interactions between the charged molecules and the charged metal surface. The chemisorption phenomenon is associated with the charge transfer from the inhibitor to the metal surface by coordinate bond, according to literature [39,40].  $\Delta G_{\text{ads}}^0$  values obtained in this work are between -42.52 and -43.75 kJ mol<sup>-1</sup>, suggesting a possible chemisorption mechanism related to the donor–acceptor interactions between the lone pairs of electrons of sulfur and nitrogen atoms,  $\pi$ -electrons of phenyl and the vacant  $d$ -orbitals of the iron atom on the steel surface [40]. The possible physisorption mechanism can be related to the protonation of the thiourea molecules in acidic solutions forming cations, thereby promoting an electrostatic interaction between the positively charged sulfur and nitrogen atoms, and the negatively charged steel surface.

### 3.5. Scanning electron microscopy (SEM)

Results of surface analyses after 2 h exposure in 1 mol L<sup>-1</sup> HCl, in the presence and absence of the best inhibitor (THIOF2), can be observed in Fig. 8. The formation of pitting corrosion was clearly observed on the carbon steel surface in the absence of an inhibitor (Blank), probably due to the presence of chloride ions in solution since it favours such formation [42,43].

Pitting formation was not observed on the carbon steel surface in the presence of the inhibitor (THIOF2), the phenomenon can be related with the adsorption of the organic inhibitor on the surface, which blocks the metal sites avoiding chloride adsorption, and consequently inhibiting pitting corrosion formation. The roughness observed in this case is likely to be due to the complex formation of the inhibitor/iron, and also due to the formation of other oxides carrying the metal passivation.

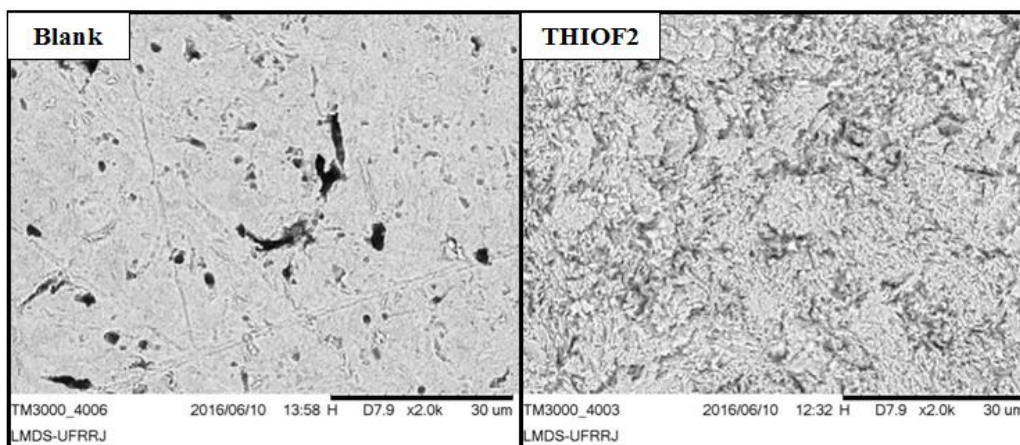


**Figure 8.** SEM micrograph (2000x) of carbon steel immersed in  $1\text{ mol L}^{-1}$  HCl in the absence (Blank) and presence of  $2.5 \times 10^{-5}\text{ mol L}^{-1}$  of THIOF2.

### 3.6. Molecular modeling

Theoretical studies of corrosion inhibitor agents have extensively been used for correlations with experimental results. In this work, the physicochemical properties of the thioureas, such as the energy of the highest occupied molecular orbital ( $E_{\text{HOMO}}$ ) and the lowest unoccupied molecular orbital ( $E_{\text{LUMO}}$ ), the Mulliken charges (MC) of sulfur atom and the dipole moment ( $\mu$ ) were calculated using semi-empirical PM3 method. All vibrational frequencies observed are real, thus the minimal energy was characterized. According to Gao and Liang, more negative charges of the heteroatom are typically related to better electron donor action [44]. It can also be observed that an increase in  $\mu$  value causes escalating corrosion inhibition efficiency, as described by Yurt *et al.* [45].

The frontier orbital theory can provide important information about corrosion inhibition efficiency. HOMO energy is associated with the ability of the molecule to donate electrons; thus, molecules with high values of  $E_{\text{HOMO}}$  tend to donate electrons more easily to  $d$  orbitals of the metal. Inversely, LUMO energy is related to the capability of the molecule to accept electrons; therefore, as  $E_{\text{LUMO}}$  decreases, the inhibitor can receive electrons from the metal more easily. Consequently, when the energy gap between HOMO and LUMO ( $\Delta E_{\text{LUMO-HOMO}}$ ) decreases, the inhibitor efficiency increases [12,13,44,46]. The quantum chemical parameters obtained can be observed in Table 5.

**Table 5.** Quantum chemical parameters of synthesized benzyl-thioureas (THIOB1-2) and phenetyl-thioureas (THIOF1-2) by semi-empirical method PM3.

Inhibitor	$E$ (eV)		$\Delta E_{\text{LUMO-HOMO}}$ (eV)	MC (eV)	$\mu$ (D)
	HOMO	LUMO			
THIOB1	-8.592	-0.660	7.932	-0.340	6.20
THIOB2	-8.546	-0.592	7.954	-0.341	6.31
THIOF1	-8.578	-0.657	7.921	-0.336	6.20
THIOF2	-8.529	-0.587	7.942	-0.341	6.44

However, this correlation of energy gap between HOMO and LUMO and Mulliken charges (MC) were not observed for benzyl-thioureas or phenethyl-thioureas, as shown in Table 5. This can be attributed to the slightly difference in corrosion inhibition efficiency of these compounds. The HOMO and LUMO orbitals can be observed in Fig. 9. The dipole moment ( $\mu$ ) presented a good correlation with inhibition efficiency, for the THIOF2, compared with other compounds.

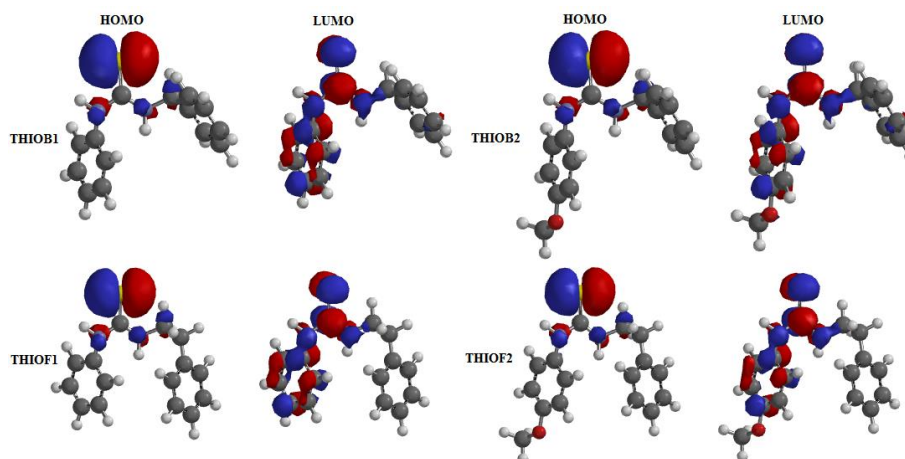


**Figure 9.** Symmetric orbitals HOMO and LUMO, for benzyl-thioureas (THIOB1-2) and phenethyl-thioureas (THIOF1-2) obtained from PM3 semi-empirical method.

#### 4. CONCLUSION

(1) All thioureas acted as good corrosion inhibitors of carbon steel in HCl 1 mol L<sup>-1</sup>. The best inhibitors were THIOF1 and THIOF2, with maximum efficiencies of 98% and 95% in 2.5x10<sup>-5</sup> mol L<sup>-1</sup>, respectively, measured by LPR.

(2) In all cases, the Nyquist plots enabled the observation of the semicircle increase as the inhibitor concentration rose.

(3) Good correlations were observed between results obtained for LPR, EIS and PP.

(4) The polarization curves showed that all the tested compounds can be classified as mixed inhibitors that reduce both the anodic and cathodic current densities, with predominant anodic effectiveness.

(5) The adsorption of THIOB 1-2 and THIOF 1-2 on a metal surface was in accordance with the Langmuir adsorption isotherm, where the correlation coefficient ranges from 0,9996 to 0,9999, and the slopes are near 1.  $\Delta G_{ads}^0$  values were in the range of -42.52 kJ mol<sup>-1</sup> to -43.75 kJ mol<sup>-1</sup>, for all thioureas.

#### ACKNOWLEDGEMENTS

The authors are very grateful to Prof. Glauco Bauerfeldt for his assistance in the molecular modeling study. The authors also thank CAPES (Coordenação de Aperfeiçoamento de Pessoal de Nível Superior), CNPq (Conselho Nacional de Desenvolvimento Científico e Tecnológico) and Petrobras (Petróleo Brasileiro S. A.), as well as P&D ANEEL-SUPERCABO project, for financial support.

## References

1. P.A. Schweitzer, Fundamentals of Corrosion: Mechanisms, Causes, and Preventative Methods (Corrosion Technology), 1<sup>st</sup> edition, CRC Press, 2009.
2. X. Li, S. Deng, H. Fu, *Corros. Sci.*, 55 (2012) 280.
3. B. Donnelly, T.C. Downie, R. Grzeskowiak, H.R. Hamburg and D. Short, *Corros. Sci.*, 18 (1978) 109.
4. S.M.A. Hosseini, A. Azimi, *Corros. Sci.*, 51 (2009) 728.
5. S.M. Abd El Haleem, S. Abd El Wanees, E.E. Abd El Aal and A. Farouk, *Corros. Sci.*, 68 (2013) 1.
6. L. Cavallaro, L. Felloni, G. Trabaneli and F. Pulidori, *Electrochim. Acta*, 8 (1963) 521.
7. I.A. Ammar and S. Darwish, *Corros. Sci.*, 7 (1967) 579.
8. B. Donnelly, T.C. Downie, R. Grzeskowiak, H.R. Hamburg and D. Short, *Corros. Sci.*, 14 (1974) 597.
9. C.B. Shen, S.G. Wang, H.Y. Yang, K. Long and F.H. Wang, *Corros. Sci.*, 48 (2006) 1655.
10. K.F. Khaled, *Appl. Surf. Sci.*, 256 (2010) 6753.
11. F.S. de Souza and A. Spinelli, *Corros. Sci.*, 51 (2009) 642.
12. V.V. Torres, V.A. Rayol, M. Magalhães, G.M. Viana, L.C.S. Aguiar, S.P. Machado, H. Orofino and E. D'Elia, *Corros. Sci.*, 79 (2014) 108.
13. C.M. Goulart, A. Esteves-Souza, C.A. Martinez-Huitle, C.J.F. Rodrigues, M.A.M. Maciel and A. Echevarria, *Corros. Sci.*, 67 (2013) 281.
14. L. Sadowski, *Arch. Civ. Mech. Eng.*, 10 (2010) 109.
15. D. Karthik, D. Tamilvendan and G. Venkatesa-Prabhu, *J. Saudi Chem. Soc.*, 18 (2014) 835.
16. M. Finšgar and J. Jackson, *Corros. Sci.*, 86 (2014) 17.
17. M.K. Awad, M.R. Mustafa and M.M.A. Elnga, *J. Mol. Struct. THEOCHEM*, 959 (2010) 66.
18. B.D. Mert, M.E. Mert, G. Kardas and B. Yazici, *Corros. Sci.*, 53 (2011) 4265.
19. I. Lukovits, A. Shaban and E. Kálmán, *Electrochim. Acta*, 50 (2005) 4128.
20. G. Gece and S. Bilgiç, *Corros. Sci.*, 51 (2009) 1876.
21. L.C.S. Aguiar, G.M. Viana, M.V.S. Romualdo, M.V. Costa and B.S. Bonato, A simple and green procedure for the synthesis of *N*-benzylthioureas, *Lett. Org. Chem.*, 8 (2011) 540.
22. P.K. Mohanta, S. Dhar, S.K. Samal, H. Ila and H. Junjappa, *Tetrahedron*, 56 (2000) 629.
23. A.R. Katritzky, S. Ledoux, R.M. Witek and S.K. Nair, *J. Org. Chem.*, 69 (2004) 2976.
24. R. Pingaew, P. Tongraung, A. Worachartcheewan, C. Nantasenamat, S. Prachayasittikul, S. Ruchirawat and V. Prachayasittikul, *Med. Chem. Res.*, 22 (2013) 4016.
25. E. Ituen, A. James, O. Akaranta and S. Sun, *Chinese J. Chem. Eng.*, 24 (2016) 1442.
26. M.A. Albuquerque, M.C.C. De Oliveira and A. Echevarria, *Int. J. Electrochem. Sci.*, 12 (2017) 852.
27. S. Şafak, B. Duran, A. Yurt and G. Türkoğlu, *Corros. Sci.*, 54 (2012) 251.
28. G. Gece, *Corros. Sci.*, 50 (2008) 2981.
29. J.J.P. Stewart, *J. Comput. Chem.*, 10 (1989) 209.
30. G. Gece and S. Bilgiç, *Corros. Sci.*, 51 (2009) 1876.
31. B. Zhang, C. He, C. Wang, P. Sun, F. Li and Y. Lin, *Corros. Sci.*, 94 (2015) 6.
32. A.B. Silva, S.M.L. Agostinho, O.E. Barcia, G.G.O. Cordeiro and E. D'Elia, *Corros. Sci.*, 48 (2006) 3668.
33. G.E. Badr, *Corros. Sci.*, 51 (2009) 2529.
34. K. Tebbji, N. Faska, A. Tounsi, H. Oudda, M. Benkaddour and B. Hammouti, *Mater. Chem. Phys.*, 106 (2007) 260.
35. M.V. Fiori-Bimbi, P.E. Alvarez, H. Vaca and C.A. Gervasi, *Corros. Sci.*, 92 (2015) 192.
36. H.M. Abd El-Lateef, *Corros. Sci.*, 92 (2015) 104.
37. M.A. Quraishi, F.A. Ansari and D. Jamal, *Mater. Chem. Phys.*, 77 (2002) 687.

38. L.A. Al Juhaiman, *Int. J. Electrochem. Sci.*, 11 (2016) 2247.
39. I. Ahamad, R. Prasad and M.A. Quraishi, *Corros. Sci.*, 52 (2010) 933.
40. M. Behpour, S.M. Ghoreishi, N. Mohammadi, N. Soltani and M. Salavati-Niasari, *Corros. Sci.*, 52 (2010) 4046.
41. A.R. Hosein-Zadeh, I. Danaee and M.H. Maddahy, *J. Mater. Sci. Technol.*, 29 (2013) 884.
42. Y. AitAlbrimi, A. AitAddi, J. Douch, R.M. Souto and M. Hamdani, *Corros. Sci.*, 90 (2015) 522.
43. A. Yurt, B. Duran and H. Dal, *Arab. J. Chem.*, 7 (2014) 732.
44. G. Gao and C. Liang, *Electrochim. Acta*, 52 (2007) 4554.
45. A. Yurt, S. Ulutas and H. Dal, *Appl. Surf. Sci.*, 253 (2006) 919.
46. T. Ghailane, R. A. Balkhmima, R. Ghailane, A. Souizi, R. Tourir, M. Ebn-Touhami, K. Marakchi and N. Komiha, *Corros. Sci.*, 76 (2013) 317.

© 2017 The Authors. Published by ESG ([www.electrochemsci.org](http://www.electrochemsci.org)). This article is an open access article distributed under the terms and conditions of the Creative Commons Attribution license (<http://creativecommons.org/licenses/by/4.0/>).